Journal of Alloys and Compounds 519 (2012) 1–3

Contents lists available at SciVerse ScienceDirect

Journal of Alloys and Compounds

journal homepage: www.elsevier.com/locate/jallcom

Letter

Improvement of magnetoelectric properties in Metglas/$Pb(Mg_{1/3}Nb_{2/3})O_3$–$PbTiO_3$ laminates by poling optimization

Yaojin Wang[a,*], David Gray[a], Junqi Gao[a], David Berry[a], Menghui Li[a], Jiefang Li[a], D. Viehland[a], Haosu Luo[b]

[a] Materials Science and Engineering, Virginia Tech, Blacksburg, VA 24061, USA
[b] Shanghai Institute of Ceramics, Chinese Academy of Sciences, 215 Chengbei Road, Jiading, Shanghai 201800, China

ARTICLE INFO

Article history:
Received 22 July 2011
Received in revised form
16 December 2011
Accepted 19 December 2011
Available online 5 January 2012

Keywords:
Magnetoelectric effect
Laminate composite
Equivalent magnetic noise
Poling

ABSTRACT

The dielectric and piezoelectric properties of ⟨0 0 1⟩-oriented $Pb(Mg_{1/3}Nb_{2/3})O_3$–$PbTiO_3$ (PMN–PT) fibers and fiber-Kapton core composites were improved by controlling their poling process. An improved poling procedure was identified for the Metglas/PMN–PT sensors, by which sensors exhibited a 1.4× enhancement in the ME coefficient, a 1.6× times reduction in the equivalent magnetic noise floor and a 1.6× times increase in magnetic field sensitivity.

1. Introduction

Multiferroics represent an appealing class of multifunctional materials that simultaneously exhibit at least two ferroic orders, such as ferroelectricity and (anti-)ferromagnetism [1,2]. The coexistence of several order parameters brings about novel physical phenomena and offers possibilities for new device functions. Of particular interest is the existence of a cross-coupling between the magnetic and electric orders, termed magnetoelectric (ME) coupling [2,3]. Since the coupling in single-phase ME materials is too low for practical device applications, intensive experimental and theoretical studies have focused on ME composites combining ferroelectric and ferromagnetic phases in two phase systems [3–7]. To date, laminated composites of magnetostrictive Metglas alloys and piezoelectric $0.7Pb(Mg_{1/3}Nb_{2/3})O_3$–$0.3PbTiO_3$ (PMN–PT) fibers operated in a multi-push–pull mode possess the largest ME effects and highest sensitivity to magnetic field variations due to their giant piezomagnetic and piezoelectric effects, respectively [8].

However, the reduction of equivalent magnetic noise and enhancement of magnetic field sensitivity is a continuous key challenge to the practical implementation of ME sensors. One strategy that might potentially address this problem is enhancing the respective individual piezomagnetic and/or piezoelectric effects in the composites [5,6]. For piezoelectric single crystals, the material properties are quite sensitive to the poling conditions. In order to gain a more comprehensive understanding on the effect of poling conditions on ME properties in Metglas/PMN–PT laminates, we explored the effects of poling procedure both on PMN–PT stand alone fibers and on PMN–PT/Metglas composite ME structures. Optimal poling conditions result in an effective improvement in the ME coefficient, a significant reduction in equivalent magnetic noise, and a notable enhancement in magnetic field sensitivity.

2. Experimental details

Commercially supplied (*Ceracomp*, Korea) PMN–PT fibers grown by a solid-state crystal growth method with dimensions and orientations of $40[1\,0\,0] \times 2[0\,1\,0] \times 0.2[0\,0\,1]\,mm^3$ were used for the present work. In order to minimize the effects of property variations owing to solute segregation during the crystal growth process, a single piece of PMN–PT fiber was chosen. After deposition of gold electrodes on the thickness surfaces, the PMN–PT was medially cut into four pieces. Each of the four samples was poled at a electric field of $E_1 = 1000\,V/mm$, but at various temperatures and with different E-field ramp rates, as detailed in Table 1. For poling procedures (a) and (b), the PMN–PT samples were poled at room temperature under a maximum E_1 for 15 min, with voltage ramp rates of +100 V/min and −20 V/min. For procedures (c) and (d), the samples were poled at 120 °C under the maximum E_1 for 15 min, then maintained at half of E_1 with $E_2 = 500\,V/mm$ during the cool down cycle. Ramp rates for procedures (c) and (d) were +100 V/min and −20 V/min for ramp-up and ramp-down, respectively. For each sample, the dielectric constant ε_r, dielectric loss tan δ, and electromechanical coupling factor k_{33} were measured or determined by an impedance analyzer (*Agilent* 4294 A), and the piezoelectric coefficient d_{33} was measured by a *Berlincount*-type meter. The parameters of the PMN–PT samples and the corresponding poling procedures are listed in Table 1. The dielectric constant of the PMN–PT fiber was

* Corresponding author. Tel.: +1 540 2316928; fax: +1 540 2318919.
E-mail addresses: yaojin@vt.edu, wangyaojin@hotmail.com (Y. Wang).

0925-8388/$ – see front matter © 2011 Elsevier B.V. All rights reserved.
doi:10.1016/j.jallcom.2011.12.093

Table 1
Poling procedures for PMN–PT fibers and their properties poled under various procedures.

Poling procedures	T (°C)	E_1 (V/mm)	E_2 (V/mm)	Ramp up/down (V/min)	ε_r [a]	tan δ [a] (%)	d_{33} [b] (pC/N)	k_{33} [c] (%)
a	25	1000	0	100	3850	2.1	920	0.74
b	25	1000	0	20	3890	1.7	980	0.76
c	120	1000	500	100	3980	1.6	1140	0.83
d	120	1000	500	20	3950	1.1	1280	0.85

[a] 16-times average method (experimental error < 1%).
[b] 5-Point average method (experimental error ~ 2%).
[c] Resonance–antiresonance method (experimental error < 1%).

insensitive to voltage ramp rate and exhibited negligible enhancement when poled at higher temperatures. Values of d_{33} and k_{33} for PMN–PT were significantly enhanced when poled at an elevated temperature of $T = 120\,^{\circ}C$ [9], due to smaller domain sizes and more neutral domain wall configurations [10,11]. However, the values of tan δ decreased both with reduced voltage ramp rate and with increasing poling temperature. This might be because during the poling process, the domain walls in PMN–PT crystals are forced to align parallel to the poling field direction: mechanical stresses will develop, which may result in microcracks within the crystals. Thus, we poled the crystal at higher temperatures and/or using slower voltage rampings: as under these conditions poling is easier thus resulting in fewer microcracks [12], and consequently lower tan δ values.

After optimizing the poling condition, two core composites were made of Kapton interdigitated copper electrodes with 300 μm wide digits spaced at 0.85 mm center-to-center (Smart Materials, USA) attached to the top and bottom sides of five $40 \times 2 \times 0.2\,mm^3$ PMN–PT fibers using epoxy resin (Stycast 1264, USA). The two Kapton/PMN–PT core composites were then poled following poling procedures (a) and (d). Commercially supplied 25 μm thick Metglas (VITROVAC7600F, nominal composition: $Fe_{74.4}Co_{21.6}Si_{0.5}B_{3.3}Mn_{0.1}C_{0.1}$, annealed at 300 °C) from Vacuumschelze (Germany) was then cut to $80 \times 10\,mm^2$ ribbons. Three such Metglas layers were then symmetrically stacked and bonded to both the top and the bottom of the two Kapton/PMN–PT fiber core composites with epoxy resin using a vacuum bag pressure method for more than 24 h at room temperature to form the Metglas/PMN–PT laminate composites [8].

3. Results and discussion

The capacitance ($C = 670$ pF, 685 pF) and dielectric loss factors (tan $\delta = 0.022$, 0.012) of the two laminates were then measured using an impedance analyzer. The DC resistance was determined to $R_{DC} = 61\,G\Omega$ and $59\,G\Omega$ for the two laminates, based on Ohm's law using the current-to-voltage data from a pA Meter/DC voltage source (HP 4140B).

The ME voltage coefficients α_E of the two Metglas/PMN–PT laminates, derivative values determined from ME charge coefficient α_Q, the capacitance (C_p) of the sensor and the length of an interdigitated unit (i.e. $\alpha_E = \alpha_Q/C_p \times l$) were characterized as a function of DC magnetic bias field H_{DC} at room temperature under zero stress bias using an in-house automated measurement system. A 1 kHz AC excitation field of $H_{AC} = 0.1$ Oe was generated by a custom-built Helmholtz coil (whose dimension is $Ø80 \times 45\,mm^3$) driven using a lock-in amplifier (SR 785). This system was calibrated by a commercial Fluxgate (FLC3-70, USA). A 5 mHz quasi-static AC voltage was applied to an electromagnet to produce the H_{DC} bias field. The H_{DC} and the induced charge/voltage synchronization signals were automatically stored in a computer. For both sensors, α_E increased with increasing H_{DC} up to about $H_{DC} = 8$ Oe, where a maximum value was reached. Above 8 Oe, α_E subsequently decreased with increase of H_{DC} as shown in Fig. 1. The maximum values of α_E for the two sensors poled using procedures (a) and (d) were 31 V/cm Oe and 42 V/cm Oe, respectively. These results demonstrate that optimal poling conditions result in an increase of α_E by a factor of 1.4×. Corresponding maximum values of α_Q were 1760 pC/Oe and 2450 pC/Oe respectively. This enhancement is a direct consequence of the increase in the piezoelectric properties originating from the optimal poling conditions.

After measuring the ME properties, the two Metglas/PMN–PT sensors were individually assembled in plastic boxes, magnetically biased using a pair of NdFeB permanent magnets, and wrapped with an EMI shielding foil. The equivalent magnetic noise floor

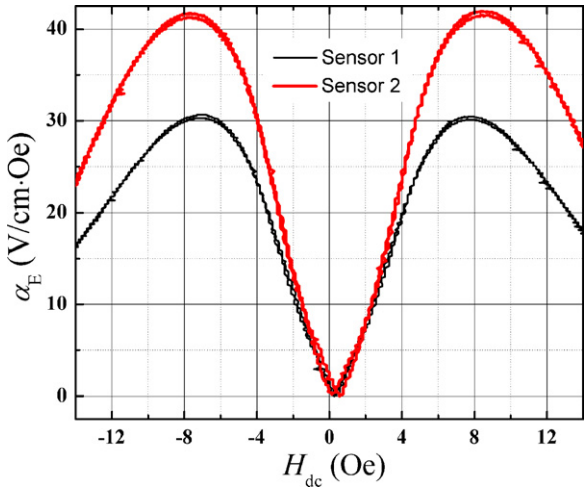

Fig. 1. ME voltage coefficient as a function of magnetic bias field for the Metglas/PMN–PT fiber heterostructures poled by different procedures: denoted as sensor #1 and sensor #2, respectively.

of the two ME laminate sensor units (sensor packages and low-noise SAIC JFET charge amplifier) was first predicted based on Eq. (1) by considering the constituent noise sources of dielectric loss (N_{DE}) and DC leakage resistance (N_R) [13], and then measured inside a high-mu-metal magnetic shielding chamber in the frequency range of $0.125 < f < 100$ Hz as shown in Fig. 2. The experimental equivalent magnetic noises of the two sensor units were deduced from the noise power spectrum in V^2/Hz directly obtained from a Dynamic Signal Analyzer (Stanford Research, SR-785), the experimental values of α_Q (in C/T), and the charge amplifier transfer

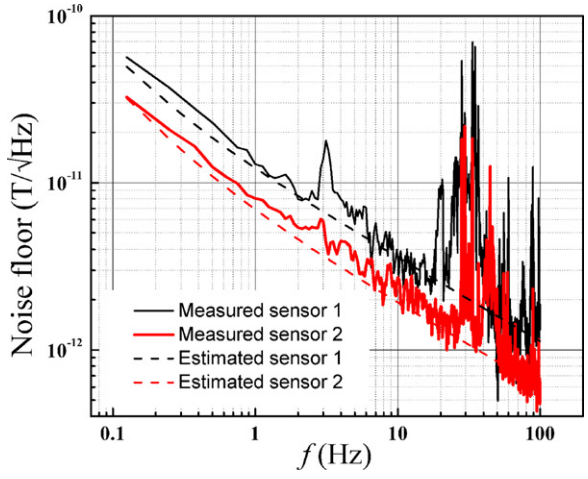

Fig. 2. Theoretical and experimental equivalent magnetic noise spectra for the two sensor units.

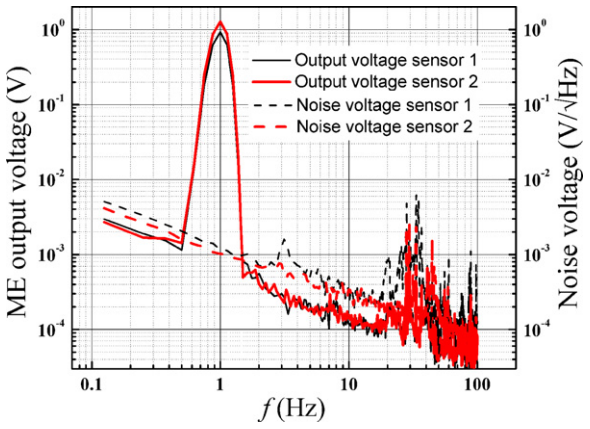

Fig. 3. ME output signals of the two sensor units in response to a 1 Hz, 10 nT incident AC magnetic field and the corresponding background noise voltage spectra observed in a zero-Gauss vibration isolation chamber in the absence of intentional excitation.

function (5.18 V/pC) [8]

$$\text{equivalent magnetic noise}\,(\text{T}/\sqrt{\text{Hz}}) = \frac{\sqrt{N_{\text{DE}}^2 + N_{\text{R}}^2}}{\alpha_{\text{Q}}}$$

$$= \frac{\sqrt{(4kTC_{\text{P}}\tan\delta/2\pi f) + (1/(2\pi f)^2)(4kT/R_{\text{DC}})}}{\alpha_{\text{Q}}}; \quad (1)$$

where k is Boltzmann's constant (1.38×10^{-23} J/K); T is temperature in Kelvin; C_{p}, $\tan\delta$ and R_{DC} are the capacitance, dielectric loss and DC resistance of the ME sensors, respectively.

In Fig. 2, it can be seen that except at frequencies where external vibration sources are present, the trend of the modeled and measured equivalent magnetic noise for each of the two sensor units shows good agreement. The experimental values are slightly higher than the theoretical values, which might be due to an over-simplification of the theoretical model in terms of electrical charge amplifier and external thermal noise sources. In particular, the experimental equivalent magnetic noises at $f = 1$ Hz for the two sensors units poled following procedures (a) and (d) were 12.9 pT/$\sqrt{\text{Hz}}$ and 8.0 pT/$\sqrt{\text{Hz}}$, respectively. A significant reduction of 1.6× in the equivalent magnetic noise was achieved solely through optimization of the poling conditions.

Finally, the magnetic field sensitivities of the two sensor units at $f = 1$ Hz were characterized in the zero-Gauss chamber through the response of the sensor to a 10 nT incident magnetic field, noise voltage V_{noise} directly obtained from the noise power spectrum, ME output voltage V_{ME} in response to the drive field, and the minimal acceptable signal-to-noise ratio (here SNR = 2) following Eq. (2) [8,13]

$$\text{magnetic field sensitivity} = \frac{H_{\text{AC}-f}}{V_{\text{ME}-f}} \times \text{SNR} \times V_{\text{noise}-f}. \quad (2)$$

Fig. 3 shows the output signals and the voltage noise spectra for both sensor units over the frequency range of $0.125 < f < 100$ Hz. Sharp V_{ME} peaks with values of 0.92 V and 1.27 V were observed at 1 Hz in response to the incident magnetic field. From the peak voltage values, the magnetic field sensitivities can be determined to be 25.2 pT and 16.1 pT, respectively. The 1.6× enhancement of magnetic field sensitivity originates from the reduction of noise voltage and improvement of the ME coefficient, resulting from the lower dielectric loss and higher piezoelectric properties by poling condition optimization.

4. Conclusions

Significant variations of the dielectric and piezoelectric properties were introduced in PMN–PT fibers and Metglas/PMN–PT sensors by adopting different poling procedures. An optimal poling procedure was employed and resulted in a 1.4× enhancement in α_{E} at 1 kHz, a 1.6× reduction in the equivalent magnetic noise floor and a 1.6× increase in the magnetic field sensitivity, compared with previous poling methods.

Acknowledgements

This work was sponsored by the DARPA and the Office of Naval Research.

References

[1] W. Eerenstein, N.D. Mathur, J.F. Scott, Nature 442 (2006) 759.
[2] M. Bibes, A. Barthelemy, Nat. Mater. 7 (2008) 425.
[3] J. Ma, J. Hu, Z. Li, C.-W. Nan, Adv. Mater. 23 (2011) 1062.
[4] M.I. Bichurin, V.M. Petrov, S.V. Averkin, E. Liverts, J. Appl. Phys. 107 (2010) 053904.
[5] Z. Min, S.W. Or, H.L.W. Chan, J. Alloys Compd. 490 (2010) L5.
[6] Y.J. Wang, S.W. Or, H.L.W. Chan, X.Y. Zhao, H.S. Luo, J. Appl. Phys. 103 (2008) 124511.
[7] Y.J. Wang, D. Gray, D. Berry, M.H. Li, J.Q. Gao, J.F. Li, D. Viehland, J. Alloys Compd. 513 (2012) 242.
[8] Y.J. Wang, D. Gray, D. Berry, J.Q. Gao, M.H. Li, J.F. Li, D. Viehland, Adv. Mater. 23 (2011) 4111.
[9] Z.Y. Feng, T.H. He, H.Q. Xu, H.S. Luo, Z.W. Yin, Solid State Commun. 130 (2004) 557.
[10] Y. Xiang, R. Zhang, W.W. Cao, J. Mater. Sci. 46 (2011) 1839.
[11] D.B. Lin, H.J. Lee, S.J. Zhang, F. Li, Z.R. Li, Z. Xu, T.R. Shrout, Scripta Mater. 64 (2011) 1149.
[12] S.Y. Chu, T.Y. Chen, I.T. Tsai, Mater. Lett. 58 (2004) 752.
[13] Y.J. Wang, D. Gray, D. Berry, J.Q. Gao, J.F. Li, D. Viehland, Phys. Status Solidi (RRL) 5 (2011) 232.